JOURNAL OF APPLIED PHYSIOLOGY
Vol. 27, No. 1, July 1969. *Printed in U.S.A.*

Effect of flow on transpulmonary circulatory transport functions

THOMAS J. KNOPP AND JAMES B. BASSINGTHWAIGHTE,
Section of Physiology, Mayo Clinic and Mayo Foundation, Rochester, Minnesota 55901

KNOPP, THOMAS J., AND JAMES B. BASSINGTHWAIGHTE. *Effect of flow on transpulmonary circulatory transport functions.* J. Appl. Physiol. 27(1): 36–43. 1969.—Lung transport functions (distributions of circulatory transit times across the lung) were characterized in four anesthetized dogs at various levels of mean pulmonary blood flow. The central circulation was found to approximate a mathematically linear, time-invariant system when respiratory frequencies were maintained at 40/min or more. Lung transport functions were obtained from 144 pairs of lung-input and lung-output dilution curves using a lumped-parameter model and an iterative convolution technique. Average relative dispersion (standard deviation of the transport function divided by mean transit time) was 0.46, about twice that found previously for segments of arteries. The relative dispersion tended to increase as the mean transit time increased, suggesting that the dispersing mechanism of the lung is dependent on the mean transit time (volume/blood flow). Differences between these results and those of single-vessel transport function studies can be resolved by considering the lung as a parallel-pathway system. It is hypothesized that, as total pulmonary blood flow increases, the pathways become more equally perfused and the relative dispersion of the lung decreases.

indicator-dilution method; central blood volume; circulatory mixing; indocyanine green; cardiac output

THE TRANSPORT FUNCTION, $h(t)$, of a segment of the circulation is the probability density function of transit times from the entrance to the exit of that segment (11, 19). Because the bolus of indicator becomes dispersed in its traversal of a segment of the circulation, any rapid fluctuations in concentration at the entrance are diminished in amplitude or slurred out during passage through the system; therefore, the system acts as a low-pass filter. It is possible to characterize this filter in mathematical terms—in terms of a model (3, 16, 20), in terms of nonparametric description as given by the transport function itself (9), or in terms of Fourier components (6).

When there is only one pathway between the upstream end of the segment and the downstream end, as in an artery, the dispersion of $h(t)$ is due to the velocity profile and to turbulence or eddies in the stream. Such transport functions have been defined for a segment of artery of the human leg (1) and also for the aorta of the dog (2). It was found that the dispersion occurring in these segments was unaffected by variations in flow rate over a wide range.

In the pulmonary vascular bed there are multiple parallel pathways and different regional perfusion rates, and it is possible that the regional pulmonary vascular volume is dependent on flow rate. The purposes of this study were to characterize the transport function of the dog's lung at various mean blood flow rates and to test the effect of changes in flow and in pulmonary blood volume on the shape of the transport function. An additional purpose was to test a new method of obtaining estimates of the fraction of the total flow passing through different regions.

METHODS

General Approach

The study has four parts: *1*) methods of obtaining the transport function, *2*) testing for applicability of superposition to transport through the lung and left side of the heart, *3*) examination of the effects of changes in lung blood flow and lung volume on the transport function, and *4*) demonstration of a new approach to the estimation of the relative flow rates through regions having different mean passage times.

The mathematical approach and the general methodology for the first two parts are essentially the same as outlined for the testing of the applicability of superposition to flow in the aorta (2). The nomenclature and mathematical terms are defined there and in Fig. 1, with the following modifications:

A = site of sampling catheter tip in main pulmonary artery
B = site of sampling catheter tip in middle of left atrium
C = site of sampling catheter tip in aorta just above aortic valve
$A(t)$, $B(t)$, $C(t)$ = concentration of indicator at sites A, B, and C at time t
$h(t)$ = transport function between two sampling points
$h'(t)$ = approximation to $h(t)$ obtained by the analysis
$h_s(t)$ = transport function of sampling systems (these were identical)
$h_i(t)$ = transport function of the ith region of the pulmonary vascular bed
f_i = (flow through the ith region)/(total pulmonary flow)
$*$ denotes the process of convolution integration
$A_s(t)$, $B_s(t)$, $C_s(t)$ = concentration recorded at time t after distortion by sampling systems
$B'_s(t)$ = computed approximation to $B_s(t)$ by $A_s(t)*h'_{AB}(t)$
$C'_s(t)$ = computed approximation to $C_s(t)$ by $B_s(t)*h'_{BC}(t)$
$C''_s(t)$ = computed approximation to $C_s(t)$ by $A_s(t)*h'_{AC}(t)$
$h''_{AC}(t)$ = computed approximation to $h_{AC}(t)$ by $h'_{AB}(t)*h'_{BC}(t)$

To assure ourselves that we obtained reasonable estimates of $h_{AB}(t)$, the focus of physiologic interest, we thought it

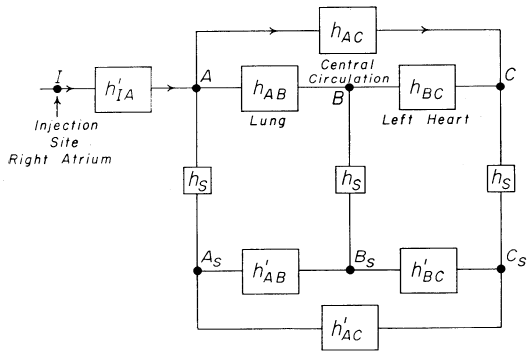

FIG. 1. Block diagram of experiment.

essential to test for the applicability of superposition in the central circulation. Deviations from linearity and stationarity were probable because *1*) flow is unsteady, *2*) the lung has multiple parallel pathways in which the relative regional distribution of flows might be expected to vary, and *3*) mixing in the left atrium and left ventricle is notoriously poor and routes of indicator transport might not be consistent from moment to moment. For these reasons the experiment was designed in a fashion similar to that used for the study of the aorta (2), so that the fundamental tests for linearity and stationarity could be done on the same data from which the transpulmonary transport functions would be estimated.

The experimental design (Fig. 1) was based on the assumption that the deviation of time-averaged sampling from volume-averaged sampling at these sampling sites is less of an error than the deviation of an experimental injection into the pulmonary artery from an ideal flow-tagging injection, as was argued previously (2). When the vascular system between A and C is linear and stationary and the sampling system transport functions are identical, then the transport functions $h'_{AB}(t)$, $h'_{BC}(t)$, and $h'_{AC}(t)$ must be identical to $h_{AB}(t)$, $h_{BC}(t)$, and $h_{AC}(t)$, respectively, in accordance with the mathematical argument given previously (1, 2). This general approach is applicable whether the transport functions are determined in terms of a model or in terms of nonparametric functions (6).

Analysis in Terms of Network of Parallel Channels

Greenleaf and associates (9) worked out a practical method for characterizing parallel-pathway systems and for obtaining estimates of relative regional transit times and flows. In its simplest form, the method requires making some assumptions about the possible forms of the transport functions, $h_i(t)$, for individual or local pathways, and it then allows one to obtain the fraction, f_i, of the total lung blood flow traversing each type of pathway. Since each individual pathway consists mostly of large vessels rather than capillaries, it seems reasonable to assume that each pathway might have a transport function similar to that found in a peripheral artery. It has been shown (1) that, over a wide range of flows, the relative dispersion and the skewness of the transport function were constant. This suggests that the transport function of each individual pathway might be described by a lagged normal density curve (or any other suitable unimodal density function) and that the transport function for the whole pulmonary circulation should be describable by the weighted sum, $\sum f_i h_i(t)$, of a family of individual transport functions of different mean transit times.

Experimental Techniques

Four mongrel dogs (21–26 kg) were anesthetized with morphine (5 mg/kg) and pentobarbital (30 mg/kg) and were studied in the left lateral position. Doses (40–60 mg) of pentobarbital were administered periodically during the study to maintain anesthesia.

The animals were intubated, and respiration with room air was maintained at 40/min with a positive-pressure (10 mm Hg) Bird respirator (Bird Oxygen Breathing Equipment, Inc., Palm Springs, Calif.) in order to obtain a high frequency of respiratory fluctuation in pulmonary blood flow and therefore minimize the error due to unsteady flow (4).

Cardiac output was varied by infusion of norepinephrine (5–50 μg/min), epinephrine (5–50 μg/min), and acetylcholine (0.06–0.62 mg/min). The drugs were infused into the arch of the aorta distal to the lungs and left heart; thus, the cardiac output was changed with changes in systemic resistance but with minimal direct action of the drugs on the pulmonary vessels or heart.

Catheters. The catheters were positioned under fluoroscopic control with monitoring of pressure. A 20-cm-long nylon cannula was positioned in the left femoral artery for measurement of aortic pressure. A 5-F NIH catheter (U.S. Catheter & Instrument Corp., Glens Falls, N.Y.), 80 cm long (volume = 0.55 ml), was introduced in the middle of the right atrium via percutaneous puncture of the left external jugular vein for injection of dye. Three identical sampling catheters (6-F, 70-cm Teflon; volume = 0.90 to 0.91 ml) were placed *1*) in the trunk of the pulmonary artery (about 2 cm above the pulmonary valve) via percutaneous introduction into the left external jugular vein, *2*) in the aortic root (about 2 cm above the aortic valve) via a cutdown on the right carotid artery, and *3*) in the middle of the left atrium via the right external jugular vein and transseptal puncture.

Indicator injections. Indocyanine green dye (150 mg) (Hynson, Westcott & Dunning, Inc., Baltimore, Md.) was mixed with 20 ml of distilled water, 97 ml of isotonic saline, and 3 ml of whole blood from the animal (to stabilize the dye solution) to give a final concentration of 1.25 mg/ml. Single injections of 1–1.3 ml were made in less than 0.26 sec, with a pneumatic injection syringe at a pressure of 12 lb./in^2. The amount of dye solution injected into the right atrium was recorded via a linear potentiometer mechanically connected in parallel with the syringe piston. The shape of the injected bolus was varied by intermixing single and double injections (a double injection is two single injections separated by 2–4 sec).

Densitometry. Waters XC100A densitometers (Waters Co., Rochester, Minn.) were used to measure the optical density of the whole blood-dye mixture at the three sampling sites simultaneously. Calibration of the densitometers was done at the beginning and end of each experiment, using five solutions of known dye concentrations (0, 5, 10, 15, and 20 mg/liter) as described previously for these instruments (8).

Sampling systems. Blood was withdrawn through the sampling systems at a rate of 24.7 ml/min with Harvard constant-infusion/withdrawal syringes (Harvard Apparatus Company, Millis, Mass.). The analytical methods demand that the three sampling systems impose equal distortion on the dye concentration-vs.-time curves. Through the three identical sampling catheters, the three Harvard syringes produced flows that were identical to within 0.5%. At the conclusion of each experiment the responses of the three sampling systems to a step change in dye concentration were obtained by using a solenoid-driven valve assembly to switch to withdrawal of blood from either of two reservoirs of solution of different concentrations (Fig. 2). The mean transit times were about 2.2 sec, and the 50% response times of the three sampling systems differed by less than 0.05 sec.

Recording system. Data were recorded as described previously (2) on analog magnetic tape (14-channel recorder, model 1200, Ampex Corp., Redwood City, Calif.) at 3.75 inches/sec and on a photokymographic record. Recorded were the three simultaneous dye-dilution curves, injection-syringe travel, right atrial pressure, pulmonary artery pressure, left atrial pressure, femoral artery pressure, airway pressure, and a binary-coded decimal signal to identify the experimental events.

Dye concentration-vs.-time curves were recorded for 60–90 sec, so that recirculation peaks were included in the dilution curves.

Data preparation. Most of the data preparation was done with a Control Data Corporation 3200 digital computer and an eight-bit analog-to-digital converter. The programming was done in Fortran II and assembly language with a Medlab time-sharing monitor modified from that developed by Pryor and Warner (14). The experimental data from the analog tape were digitized at 15 samples/sec and stored on digital magnetic tape and on IBM punched cards. The amount of dye injected (mg) was calculated from the syringe-travel signal deflection (v) times the syringe-travel calibration factor (ml/v) times the injectate dye concentration (mg/ml). The recorded densitometer curves were converted to units of milligrams per liter vs. time by using calibration factors obtained from the five known concentrations.

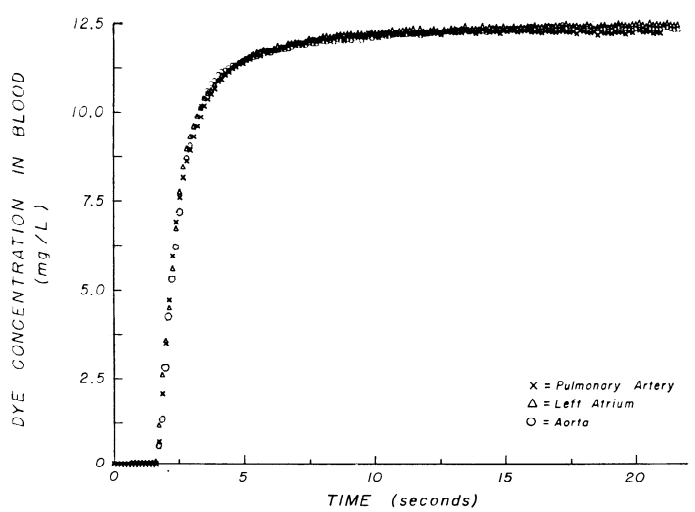

FIG. 2. Responses of three sampling systems to step changes in dye concentration at tip of catheter sampling system.

Obtaining Optimized Transport Function

The transport functions between each of the pairs of sampling sites were estimated in terms of a four-parameter equation, the lagged normal density curve as described previously (1, 3), and modified by approximating the rising slope of the distribution function with a straight line as used for aortic transport functions (6). The parameters are σ, the standard deviation, t_c, the median of the random dispersion process (Gaussian curve), τ, the time constant of the superimposed washout or lag process, and a gain factor which is ordinarily 1.0 when no indicator is lost in the circulatory segment under study. Certainly, this is not the only model that could be used, but it will be shown that this model is adequate for providing descriptions of $h(t)$. As in the previous studies, a satisfactory description of $h(t)$ was considered to have been obtained when the convolution of an unextrapolated recorded input curve, including recirculation, with a guessed trial transport function provided a theoretical output curve which closely approximated the unextrapolated recorded output curve for that segment. For each such transport function the trials were repeated up to 50 times or until the coefficient of variation between the observed and computed downstream curves was less than 0.01. The convolution integration was performed numerically by using Simpson's-rule integration.

A test of the optimization of the fitting of the theoretical recorded curves (e.g., the fitting of $B'_s(t)$ to $B_s(t)$) and a test of the convergence of the method used to adjust the parameters of the model for each iteration were examined by mapping the coefficient of variation between $B'_s(t)$ and $B_s(t)$ above a plane defined by the parameters of the model. The mapping in this plane allowed us to observe whether there were valleys having a coefficient of variation relatively high compared to the best obtainable fit in which the solution might become trapped or whether the surface was unimodal and steeply pitched so that an optimum was obtained with some precision. The most useful planes tested were the σ, τ plane and the dispersion, mean transit time plane. The former is the plane of the two dispersive parameters of the lagged normal density curve, but the latter is more general.

Figure 3 shows the three-dimensional plot of the coefficient of variation between a recorded and a theoretical output curve as a function of the dispersion and of the mean transit time of the assumed transport function. It is seen that, over a wide region in this plane, the surface has a simple, smooth shape, with a well-delineated hill with reasonably steep sides in the region approaching the best set of parameters. In this domain, using this model, the region of best fit is clearly defined, so simple optimization procedures sufficed to obtain convergence toward a best, and nearly unique, solution. This rather satisfying result was shown for each set of the curves examined. The smallness of the coefficient of variation at the peak of the hill provides reasonable assurance that the values obtained for the transport function are not only the best description but also a good description.

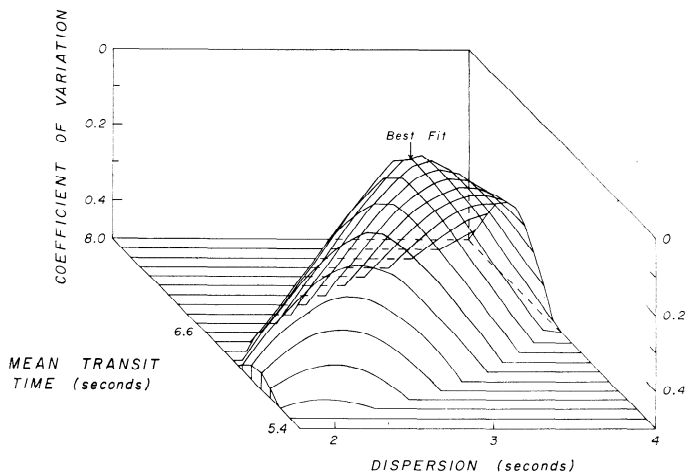

FIG. 3. Three-dimensional plot of closeness of fit of $B'_s(t)$ to $B_s(t)$ (coefficient of variation) as function of mean transit time and dispersion of transport function. "Best fit" is indicated by peak of hill where coefficient of variation is minimal, 0.045; $\bar{t}$ is 6.8 sec and dispersion is 3.1 sec. All values of coefficient of variation greater than 0.5 were arbitrarily set to 0.5.

Calculations of Pulmonary Blood Flow and Volume

Three estimates of pulmonary blood flow were obtained from the three simultaneously recorded dye-dilution curves by the Stewart-Hamilton technique with monoexponential extrapolation of the downslopes. The mean flow, F, was the average of the three estimates. Differences between the three flow estimates appear to occur randomly with respect to sampling site. The mean difference in flows calculated from curves sampled at the pulmonary artery and the left atrium was 0.08 liter/min (SD = 0.57). The mean difference for pulmonary artery and aorta sampling was 0.12 liter/min (SD = 0.58). Much of the difference was attributable to inaccuracies in densitometer calibration factors. By assuming that the mean difference between the flows at the two sites was zero for each experiment, multiplication of the calibration factor for the pulmonary artery densitometer by the mean ratio of flows at the left atrium and pulmonary artery resulted in a reduction of the standard deviation of the difference to 0.26 liter/min. In any case, errors in the densitometer calibrations did not change the shape of the dye-dilution curves and, hence, did not affect the transport function approximations. The cause of the residual variation is unknown, but it seems likely that it is related, at least in part, to the extrapolation performed on the downslopes of the curves. The flow calculations were dependent on this extrapolation to remove the effects of recirculating dye, but the recorded, unextrapolated curves were used to compute the transport functions, which obviates this source of error. $\bar{t}_{h'_{AB}(t)}$, the mean transit time of $h'_{AB}(t)$, was considered to be the transpulmonary mean transit time. The estimate of transpulmonary blood volume, V, was the product of F and $\bar{t}_{h'_{AB}(t)}$. This estimate contains a portion of the left atrial volume.

Parallel-Pathway Analysis

Individual pathway transport functions, $h_i(t)$, were assumed to have a relative dispersion of 0.2 and a skewness of 1.0, similar to that found for a single branching vessel (1). Relative dispersion is the square root of the variance of $h_i(t)$ divided by its mean transit time, $\bar{t}_{h_i(t)}$; for the lagged normal density curve the relative dispersion is $\sqrt{\sigma^2 + \tau^2}/(\tau + t_c)$. Considering this set, or family, of transport functions as an orthogonal domain, the frequency of occurrence of each member of the family was ascertained and the result was checked by comparing the weighted sum to the transport function, $h'_{AB}(t)$, or by using the weighted sum as the transport function itself and testing the convolution of this transport function with the input curve, $A_s(t)$, to obtain a theoretical left atrial curve, $B'_s(t)$, for comparison with the recorded left atrial curve, $B_s(t)$.

RESULTS

Test of Applicability of Superposition to Central Circulation

Figure 4 shows the type of data obtained for the test of linearity. One set of original data, the three dilution curves, $A_s(t)$, $B_s(t)$, and $C_s(t)$, recorded following one dye injection, is shown in the left upper panel. A similar set is shown in the left lower panel; 144 sets of such recordings were obtained at different flow rates and under different physiologic situations in four dogs.

Superimposed on $B_s(t)$ is $B'_s(t)$ which is $h'_{AB}(t)*A_s(t)$; the closeness of the fit between $B_s(t)$ and $B'_s(t)$ is quantitated in terms of the coefficient of variation (0.056 in the upper panel) and gives an indication of the accuracy of $h'_{AB}(t)$. $C'_s(t)$ and $C''_s(t)$ are also closely approximated to $C_s(t)$, showing that $h'_{BC}(t)$ and $h'_{AC}(t)$ were good descriptions of $h_{BC}(t)$ and $h_{AC}(t)$. The closeness of fit between the curves in the upper panel was representative of the average for the whole experiment; the closeness in the lower panel was better than average. The average coefficient of variation of $B'_s(t)$ to $B_s(t)$ and $C'_s(t)$ to $C_s(t)$ was 0.056 (SD = 0.021; N = 288).

The test for the applicability of superposition is given in the right panels. $h''_{AC}(t)$ is seen to approximate $h'_{AC}(t)$ closely. For 113 sets of three recorded curves, the coefficient of variation between $h''_{AC}(t)$ and $h'_{AC}(t)$ averaged 0.178 (SD = 0.075). The relationships between the mean transit time of $h''_{AC}(t)$ and a standard deviation of $h''_{AC}(t)$ against the same parameters of $h'_{AC}(t)$ are shown in Fig. 5. The coefficients of variation and the data of Fig. 5 show that better fits were obtained between $h''_{AC}(t)$ and $h'_{AC}(t)$ in this central circulatory system than were obtained for the dog's aorta (2) and therefore justify the conclusion that, for all practical purposes, the system may be considered to be linear and stationary over the periods of recording dilution curves under the specific circumstances of anesthesia and ventilatory and cardiac rates obtained in these dogs.

Transpulmonary Transport Functions

One hundred forty-four lung transport functions were approximated by the lagged normal density curve model. The mean coefficient of variation between $B_s(t)$ (the recorded curve sampled at the left atrium) and $B'_s(t)$ (the convolution of the recorded curve sampled at the pulmonary artery and the transport function) was 0.058 (SD = 0.019), indicating the appropriateness of the model.

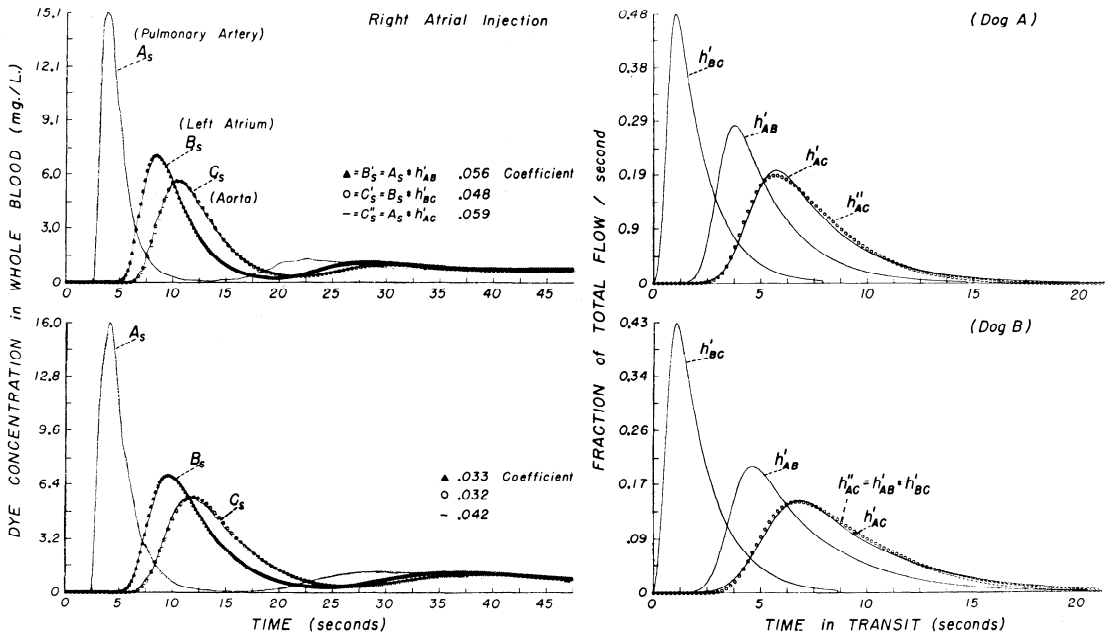

FIG. 4. Test for applicability of superposition to central circulation. *Left panels* show two sets of experimental indicator-dilution curves. Superimposed on recorded downstream curves, $B_s(t)$ and $C_s(t)$, are theoretical curves, $B'_s(t)$, $C'_s(t)$, and $C''_s(t)$, obtained by convolution of input function with estimated transport function. *Right panels* show associated two sets of three transport functions. Superimposed on $h'_{AC}(t)$ is $h''_{AC}(t)$, showing close correspondence of these two and illustrating that central circulation can be considered as linear, stationary system.

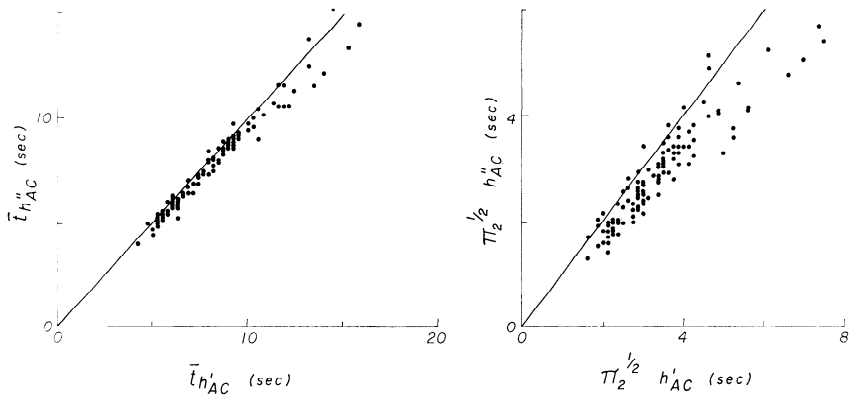

FIG. 5. Comparison of mean transit times (*left panel*) and standard deviations (*right panel*) of $h''_{AC}(t)$ and $h'_{AC}(t)$. Equation for data in *left panel* is $\bar{t}_{h''_{AC}(t)} = 0.29 + 0.92\ \bar{t}_{h'_{AC}(t)}$ (N = 113; r = 0.986); for *right panel*, $\pi_2^{1/2}h''_{AC}(t) = 0.24 + 0.79\ \pi_2^{1/2}h'_{AC}(t)$ (N = 113; r = 0.93), in which $\pi_2^{1/2}$ is the standard deviation of $h(t)$. The lines of identity are drawn in.

Figure 6 illustrates the changes in the transport function (labeled $h'_{AB}(t)$ or $h'(t)$) as the cardiac output in one dog was decreased to less than half of its original value. The transport function is scaled to an arbitrary peak but has the correct time scale. In all the dogs, as the mean flow decreased, the temporal dispersion in the circulation increased and there was an increasing difference between the recorded curve sampled from the pulmonary artery and the recorded curve sampled from the left atrium. This is apparent in the increasing width of the lung transport function, $h'_{AB}(t)$. In Fig. 6 the mean transit time of the lung transport function changed from 2.9 sec at a flow of 4.2 liters/min to 6.8 sec at a flow of 2.0 liters/min and was approximately inversely related to the flow.

The mean transit time, $\bar{t}$, and the dispersion, $(\sigma^2 + \tau^2)^{\frac{1}{2}}$, are related as shown in Fig. 7. The linear regression equation is $(\sigma^2 + \tau^2)^{\frac{1}{2}} = 2.65\ \bar{t} - 1.10, (r = 0.94)$; but, since the intercept is not zero, the relative dispersion is dependent on the transit time, being larger with large mean transit times. The mean relative dispersion is 0.46 (SD = 0.06). This large relative dispersion—more than twice the value found in large arteries of the human leg (1)—suggests that the mechanism of dispersion in the pulmonary circulation is different from that in large arteries. A similar conclusion was made from the data obtained in humans (1), which showed that the relative dispersion occurring from the root of the aorta to the dorsalis pedis artery was less than the relative dispersion occurring between the superior vena cava and the dorsalis pedis artery. Since the pulmonary circulation is a complex arrangement of parallel pathways, the dispersion could be a function of the distribution of pathway lengths or flows as well as of the dispersion within each of the individual vessels.

Changes in absolute temporal dispersion are expected with changes in either flow or volume but, if changes in volume induced changes in flow characteristics or changes

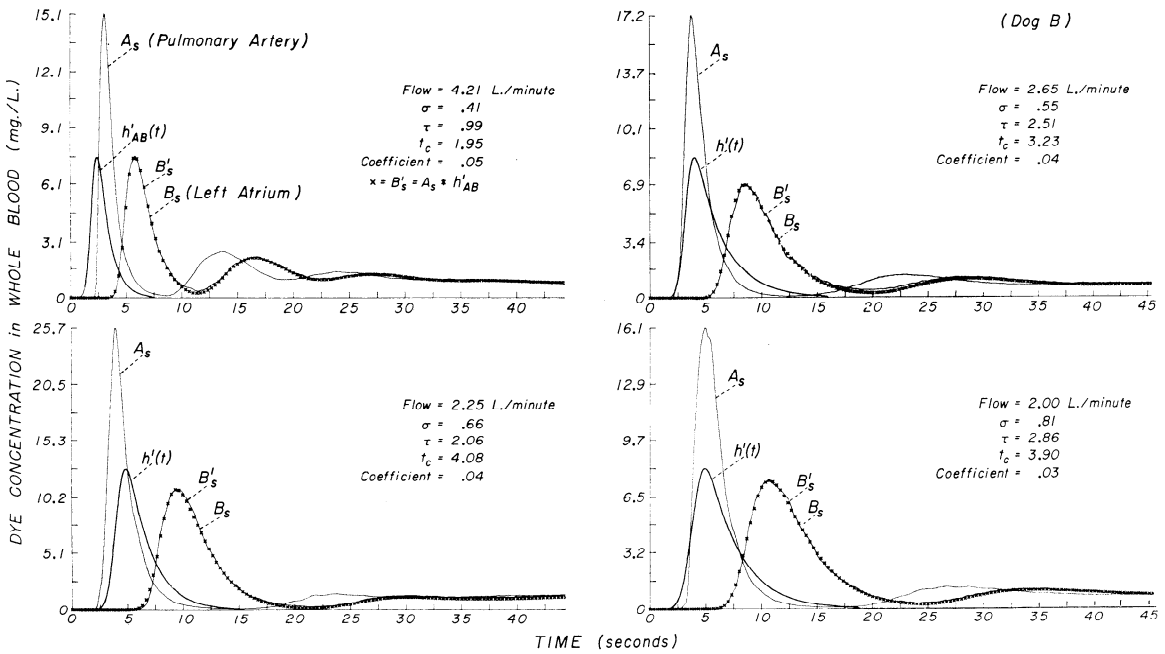

FIG. 6. Effect of flow rate on transpulmonary circulatory transport functions. In each panel are shown dye curves from pulmonary artery and left atrium and the transport function, $h'_{AB}(t)$. Comparison of transport functions at four different flow rates in one animal shows that there is increased temporal dispersion at decreased flow. Parameters of each transport function are given.

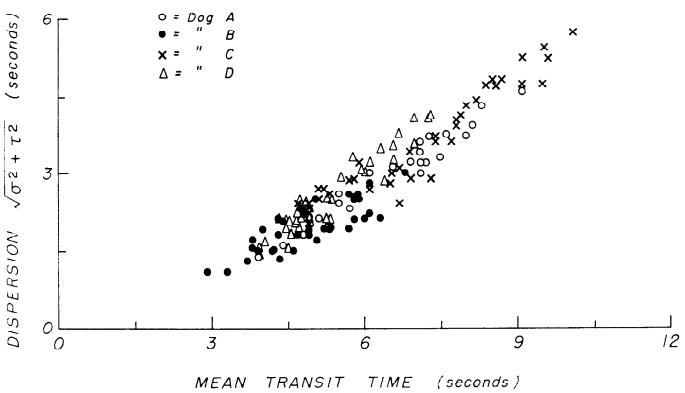

FIG. 7. Relationship of transpulmonary mean transit time to dispersion of transport function. Data for four experiments are shown. It is apparent that relationship is not linear through origin and that there is mildly increased relative dispersion at low flow rates (long mean transit times).

in flow were accompanied by changes in relative regional perfusion rates, then the relative dispersion might also change as a function of pulmonary blood flow or volume. The correlation of relative dispersion with flow gave $r = -0.26$ and with volume, $r = +0.22$, but with mean transit time, $r = 0.49$, showing that both flow and volume influence relative dispersion.

Analysis in Terms of Parallel Pathways

The transport function for a single pathway through the lung could be represented by three serial components: *1)* pulmonary arterial system, *2)* capillary, *3)* pulmonary venous system. The capillaries comprise only a very small part of this system and, because relative dispersion in a single artery or vein is about 0.2, it is apparent that the major source of dispersion is the variety of path lengths and blood velocities in different pathways. A parallel-pathway model was therefore synthesized in which the delay and dispersion of each pathway, or class of pathways with similar transit times, was approximated with a lagged normal density curve. This is similar to that which Nicholes and associates (12) used for the systemic circulation.

The lower panel of Fig. 8 shows the parallel-pathway model applied to a lung transport function, $h(t)$. Each individual transport function, $h_i(t)$, is defined by having a constant relative dispersion equal to 0.2 and skewness equal to 1.0 and is describable by a lagged normal density curve $[\sqrt{\sigma^2 + \tau^2}/(\tau + t_c) = 0.2; \beta_1 = 1.0]$. Twenty members

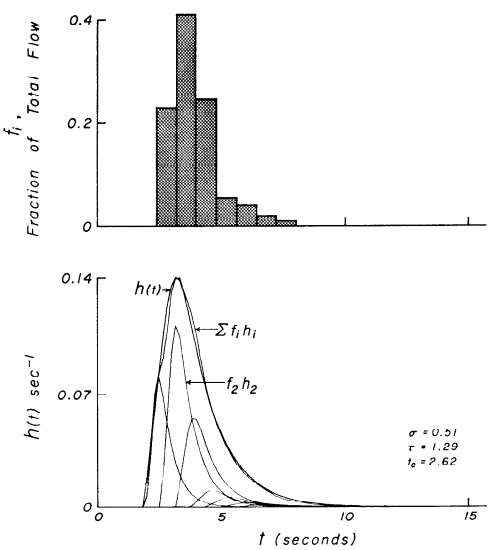

FIG. 8. Description of transport function through pulmonary circulation by family of transport functions having relative dispersion and skewness similar to those found for single vessels (cardiac output, 4.7 liters/min).

of the family were assumed to define a full set, each member being describable by its mean transit time, $\bar{t}$. The relative occurrence of each member of this family for a particular transport function is given in the upper panel of Fig. 8, where f_i is the fraction of the total blood flow having a particular $\bar{t}$. The total transpulmonary transport function is the weighted sum of the members of the family, $\sum f_i h_i(t)$, and is shown in the lower panel in comparison with $h(t)$ as obtained via the convolution technique.

It is expected that, as mean blood flow and pulmonary blood volume vary, this model will make obvious any shifts in blood flow from one class of pathways to another. Perhaps the inconstancy of the relative dispersion exhibited by the lung transport function can be explained by these changes in regional perfusion.

DISCUSSION

The lagged normal density equation was used to model the circulatory transport function of the lung because it was previously found to describe transport functions of the arterial circulation (1–3) and because its four parameters lend themselves to simple logical adjustments to obtain good approximations. Good descriptions of the transport function were obtained for 144 sets of curves in spite of up to fourfold variations in mean blood flow rate. Good fits were also obtained with the model applied to the transport function of the left side of the heart and to the whole central circulation (coefficient of variation for $C'_s(t)$ and $C_s(t)$ was $0.054 \pm .023$ and for $C''_s(t)$ and $C_s(t)$, $0.050 \pm .018$).

The entire structure of the data analysis was dependent on the applicability of the convolution integral, i.e., the system must be linear and stationary. Though it is clear that this pulsatile flow system is not stationary, the close similarity between $h'_{AC}(t)$ and $h''_{AC}(t)$ suggests that the system is functionally stationary and that the fluctuations in flow can be considered as noise in a steady-flow system. A theoretical study (4) has shown quantitatively that this should be so. That is, for systems having a mean transit time of 3 sec and a relative dispersion of about 0.46, less than 10% error in area and dispersion should result when the heart rate is 90/min or more; errors due to a heart rate of 80/min or greater would be less than 2% when $\bar{t}$ is 6 sec or more.

Since $h(t)$ was apparently adequately described by the model, its parameters could be examined with regard to the induced changes in pulmonary blood volume and blood flow. In single-vessel systems, the relative dispersion was much less than obtained here for the lung; in a peripheral artery (1) it was 0.18 and in the aorta it was about 0.28. Dispersion across the lung differed in two ways: *1*) the average relative dispersion was 0.46 and *2*) it was not constant when the mean blood flow and lung blood volume were altered. Sheppard and associates (18) have approximated the central circulatory transport function with a random-walk equation. Their value, 0.35, for the relative dispersion is less than our average value but is similar to our values obtained at increased cardiac output.

Since sampling site B was at the middle of the left atrium, the so-called transpulmonary volume contains a portion of left atrial volume, and, because of the inconsistency of mixing at this site, this portion is not accurately known and may be variable. Nevertheless, since the atrial volume is only about 15–20 ml in these dogs, the overestimation of pulmonary blood volume will be small and is partially or completely compensated for by having the upstream sampling site, A, about 2 cm above the pulmonary valve. The error is almost certainly less than might be obtained by sampling either one or two of the pulmonary veins, because transit times through one pulmonary region may be quite different from those through another.

Other methods for measuring pulmonary transport functions have been used. One such is the simultaneous injection of two different indicators into the pulmonary artery and the left atrium with sampling for both indicators at a downstream site (5). While this clearly makes the sampling systems identical, the approach is based on the invalid assumption of similar mixing characteristics at the two injection sites. It is difficult to know how great the errors might be. Injection into an artery appears to produce a more or less cross-sectional labeling of the fluid and therefore a disproportionate amount is injected into the lower-velocity streams near the wall. The angiographic appearance of an atrial injection suggests that deviations from flow tagging may be much greater with atrial than with arterial injections because large fractions of the indicator may be suspended in slow-moving streams near the atrial wall, causing large prolongations of the estimated mean transit time. Error in the estimation of volume is very dependent on the accuracy of the estimates of flow and mean transit time and may be larger than the error in either (4, 17). Our estimates of pulmonary blood volume are presumably of least accuracy at high flows since errors due to cardiac and respiratory fluctuations in flow are maximal at short mean transit times (4), but there was no significant increase in the coefficients of variation when transit times were short.

The large value for the relative dispersion can best be explained in terms of the many parallel pathways through the lung and a heterogeneity of pathway mean transit times. Differences in regional perfusion in the lung have been demonstrated by others (10, 21). Redistribution of lung blood flow accompanies environmental changes such as changes in direction and magnitude of gravitational forces (15). The lung capillaries have low compliance, and large changes in total lung blood flow are accompanied by relatively small changes in pulmonary blood volume (7). It is quite likely that some previously closed pathways open when total blood flow is increased by increasing the perfusion pressure (5). But changes in regional perfusion due to increases in total blood flow are also likely to be a result of a more equal perfusion of previously open pathways. The latter explanation is more compatible with our observation of increased relative dispersion at long mean transit times (Fig. 7). Our data from these intact, closed-chest dogs do show that increased dispersion accompanied decreased left atrial pressure, just as Permutt and Maseri (personal communication) found in isolated perfused lungs. Although not performed routinely, a few simultaneous determinations of relative dispersion and left atrial pressure gave a mean of -0.023 as the slope of relative dispersion vs. pressure ($N = 9$; $r = -0.74$).

The parallel-pathway concept was applied to the lung

previously by Parrish and co-workers (13) who used cascaded dispersive delay lines to describe the pulmonary functions. Lenfant and Okubo (10) used an interesting parallel-pathway model for uptake of O_2 by the lung. The O_2 was assumed to be washed out of the individual alveoli in a double-exponential manner in which the O_2 concentration in the alveoli is dependent on ventilation and the rate of washout is dependent on blood flow. Their model assumed nondispersive plug flow from the alveoli to the brachial artery, but we find it preferable to use transport function models which include both dispersion and delay along each pathway.

This investigation was supported, in part, by Research Grants HE-9719, HE-4664, and FR-7 from the National Institutes of Health.

J. B. Bassingthwaighte is recipient of a National Institutes of Health Career Development Award.

Received for publication 16 March 1969.

REFERENCES

1. Bassingthwaighte, J. B. Plasma indicator dispersion in arteries of the human leg. *Circulation Res.* 19: 332–346, 1966.
2. Bassingthwaighte, J. B., and F. H. Ackerman. Mathematical linearity of circulatory transport. *J. Appl. Physiol.* 22: 879–888, 1967.
3. Bassingthwaighte, J. B., F. H. Ackerman, and E. H. Wood. Applications of the lagged normal density curve as a model for arterial dilution curves. *Circulation Res.* 18: 398–415, 1966.
4. Bassingthwaighte, J. B., and T. J. Knopp. Effects of unsteady flow on indicator dilution in the circulation. *Circualtion Res.* In press.
5. Caldini, P., S. Permutt, and A. Maseri. Effect of pulmonary vascular pressures and blood flow on CO diffusing capacity. (Abstract). *Federation Proc.* 27: 379, 1968.
6. Coulam, C. M., H. R. Warner, H. W. Marshall, and J. B. Bassingthwaighte. A steady-state transfer function analysis of portions of the circulatory system using indicator dilution techniques. *Computers Biomed. Res.* 1: 124–138, 1967.
7. De Freitas, F. M., E. Z. Faraco, D. F. de Azevedo, J. Zaduchliver, and I. Lewin. Behavior of normal pulmonary circulation during changes of total blood volume in man. *J. Clin. Invest.* 44: 366–378, 1965.
8. Edwards, A. W. T., J. Isaacson, W. F. Sutterer, J. B. Bassingthwaighte, and E. H. Wood. Indocyanine green densitometry in flowing blood compensated for background dye. *J. Appl. Physiol.* 18: 1294–1304, 1963.
9. Greenleaf, J. F., T. J. Knopp, C. M. Coulam, and J. B. Bassingthwaighte. Identification of parallel pathway systems. (Abstract). *Proc. Ann. Conf. Eng. Med. Biol., 21st, Houston* 10: 50.6, 1968.
10. Lenfant, C., and T. Okubo. Distribution function of pulmonary blood flow and ventilation-perfusion ratio in man. *J. Appl. Physiol.* 24: 668–677, 1968.
11. Meier, P., and K. L. Zierler. On the theory of the indicator-dilution method for measurement of blood flow and volume. *J. Appl. Physiol.* 6: 731–744, 1954.
12. Nicholes, K. K., II. R. Warner, and E. H. Wood. A study of dispersion of an indicator in the circulation. *Ann. N.Y. Acad. Sci.* 115: 721–737, 1964.
13. Parrish, D., D. T. Hayden, W. Garrett, and R. L. Huff. Analog computer analysis of flow characteristics and volume of the pulmonary vascular bed. *Circulation Res.* 7: 746–752, 1959.
14. Pryor, A., and H. R. Warner. Time-sharing. In: *Datamation*, edited by J. Moshman. Washington, D. C.: Thompson, 1966, p. 54.
15. Reed, J. H., Jr. *The Distribution of Pulmonary Blood Flow (The Influence of Gravity and Increased Inertial Force Environments)* (Ph.D. thesis). Rochester, Minn.: Mayo Graduate School of Medicine (University of Minnesota), 1967.
16. Sheppard, C. W. Mathematical considerations of indicator dilution techniques. *Minn. Med.* 37: 93–104, 1954.
17. Sheppard, C. W. An electromathematical theory of circulatory mixing transients. In: *Proceedings of the First National Biophysics Conference.* New Haven, Conn.: Yale Univ. Press, 1959, p. 476–492.
18. Sheppard, C. W., M. B. Uffer, P. C. Merker, and G. Halikas. Circulation and recirculation of injected dye in the anesthetized dog. *J. Appl. Physiol.* 25: 610–618, 1968.
19. Sherman, H. On the theory of indicator-dilution methods under varying blood-flow conditions. *Bull. Math. Biophys.* 22: 417–424, 1960.
20. Thompson, H. K., Jr., C. F. Starmer, R. E. Whalen, and H. D. McIntosh. Indicator transit time considered as a gamma variate. *Circulation Res.* 14: 502–515, 1964.
21. West, J. B. Distribution of gas and blood in the normal lungs. *Brit. Med. Bull.* 19: 53-58, 1963.